

Benchmark tests on pressure boundary conditions

Francesco Parisio^a, Dmitry Naumov^a, Thomas Nagel^{a,b}

^a*Department of Environmental Informatics, Helmholtz Centre for Environmental Research – UFZ, Leipzig, Germany*

^b*Department of Mechanical and Manufacturing Engineering, School of Engineering, Trinity College Dublin, College Green, Dublin, Ireland*

1. Analytical solutions

In the following are reported the formula relatives to the analytical solutions of the stress and displacement fields around a thick-walled pipe and sphere in elastic conditions and a thick walled sphere in elasto-plastic conditions. The full derivation of the analytical solutions can be found in [1].

1.1. Thick-walled elastic cylinder

The stress field around a thick walled elastic cylinder in plain strain conditions is expressed by the set of equations

$$\sigma_{rr} = \frac{p_i R_i^2 - p_a R_a^2}{R_a^2 - R_i^2} - \frac{(p_i - p_a) R_a^2 R_i^2}{(R_a^2 - R_i^2) r^2}, \quad (1)$$

$$\sigma_{\theta\theta} = \frac{p_i R_i^2 - p_a R_a^2}{R_a^2 - R_i^2} + \frac{(p_i - p_a) R_a^2 R_i^2}{(R_a^2 - R_i^2) r^2}, \quad (2)$$

$$\sigma_{zz} = 2\nu \frac{p_i R_i^2 - p_a R_a^2}{R_a^2 - R_i^2}, \quad (3)$$

defining the radial σ_{rr} , circumferential $\sigma_{\theta\theta}$ and longitudinal σ_{zz} stress components in cylindrical coordinates, where the z axis is along the cylinder directive. The thick walled cylinder is subjected to an internal and an external pressure, respectively p_i and p_a , and has internal and external radii of R_i and R_a . The radial coordinate is r and ν is Poisson's ratio. The radial displacement u_r writes

$$u_r = \frac{R_i^2 p_i (1 + \nu) r}{E (R_i^2 - R_a^2)} \left\{ \left[\frac{p_a}{p_i} \left(\frac{R_a}{R_i} \right)^2 - 1 \right] (1 - 2\nu) + \left(\frac{p_a}{p_i - 1} \right) \left(\frac{R_a}{r} \right)^2 \right\} \quad (4)$$

where E is Young's modulus.

1.2. Thick-walled elastic sphere

The stress field around a thick walled elastic sphere of internal and external radii R_i and R_a , respectively, and subjected to and internal and external pressure of p_i and p_a , respectively, is given by

$$\sigma_{rr} = \frac{p_a R_a^3 - p_i R_i^3}{R_i^2 - R_a^2} - \frac{(p_a - p_i) R_a^3 R_i^3}{(R_i^3 - R_a^3) r^3}, \quad (5)$$

$$\sigma_{\theta\theta} = \sigma_{\phi\phi} = \frac{p_a R_a^3 - p_i R_i^3}{R_i^2 - R_a^2} + \frac{(p_a - p_i) R_a^3 R_i^3}{2 (R_i^3 - R_a^3) r^3}, \quad (6)$$

where in spherical coordinates, θ and ϕ define the angular coordinates and r the radial one. The radial displacement field writes

$$u_r = \frac{R_i^3 p_i r}{E (R_i^3 - R_a^3)} \left\{ \left[\frac{p_a}{p_i} \left(\frac{R_a}{R_i} \right)^3 - 1 \right] (1 - 2\nu) + \left(\frac{p_a}{p_i} - 1 \right) \frac{1 + \nu}{2} \left(\frac{R_a}{r} \right)^3 \right\}. \quad (7)$$

1.3. Thick walled plastic sphere

The solution obtained is based on perfect plasticity theory (no hardening or softening) and the Von Mises plastic yield surface F , which reads

$$F = \frac{1}{2} s_{ij} s_{ij} - \frac{1}{3} \sigma_F^2 = 0, \quad (8)$$

where $s_{ij} = \sigma_{ij} - 1/3 \sigma_{kk} \delta_{ij}$ is the deviatoric stress tensor and σ_F is the yield stress. A new variable r_p defines the boundary between the elastic and the plastic region and the yield pressure reads

$$p_{pl} = 2\sigma_F \ln \frac{r_p}{R_i} + \frac{2}{3} \sigma_F \left[1 - \left(\frac{r_p}{R_a} \right)^3 \right]. \quad (9)$$

In the elastic region, the stress components are

$$\sigma_{rr} = \frac{2}{3} \sigma_F \left[\left(\frac{r_p}{R_a} \right)^3 - \left(\frac{r_p}{r} \right)^3 \right], \quad (10)$$

$$\sigma_{\theta\theta} = \sigma_{\phi\phi} = \frac{2}{3} \sigma_F \left[\left(\frac{r_p}{R_a} \right)^3 + \frac{1}{2} \left(\frac{r_p}{r} \right)^3 \right], \quad (11)$$

and the radial displacement is

$$u_r = \frac{2\sigma_F}{3E} \left(\frac{r_p}{R_a}\right)^3 r \left[(1 - 2\nu) + \frac{1 + \nu}{2} \left(\frac{r_a}{r}\right)^3 \right]. \quad (12)$$

In the plastic region, stress components write

$$\sigma_{rr} = 2\sigma_F \ln \frac{r_p}{R_i} + \frac{2}{3}\sigma_F \left[\left(\frac{r_p}{R_a}\right)^3 - 1 \right], \quad (13)$$

$$\sigma_{\theta\theta} = \sigma_{\phi\phi} = 2\sigma_F \ln \frac{r_p}{R_i} + \frac{2}{3}\sigma_F \left[\left(\frac{r_p}{R_a}\right)^3 + \frac{1}{2} \right], \quad (14)$$

while the radial displacement is

$$u_r = \frac{2(1 - 2\nu)\sigma_F}{3E} r \left[\frac{3(1 - \nu)}{2(1 - 2\nu)} \left(\frac{r_p}{r}\right)^3 - 1 + \left(\frac{r_p}{R_a}\right)^3 + 3 \ln \left(\frac{r}{r_p}\right) \right]. \quad (15)$$

2. Numerical analyses and comparison

2.1. Elastic cylinder

The solution was obtained with the values reported in Table 2.1. The comparison between analytical and numerical solution is reported in Figure 1 for plain strain conditions and in Figure 2 for axisymmetric conditions. The numerical solution matches well the analytical ones.

Table 1: Values of parameters for elastic cylinder problem.

| Parameter | Value | Units |
|-----------|-------|-------|
| R_i | 1 | mm |
| R_a | 2 | mm |
| p_i | 52.2 | MPa |
| p_a | 0.1 | MPa |
| ν | 0.3 | - |
| E | 210 | GPa |

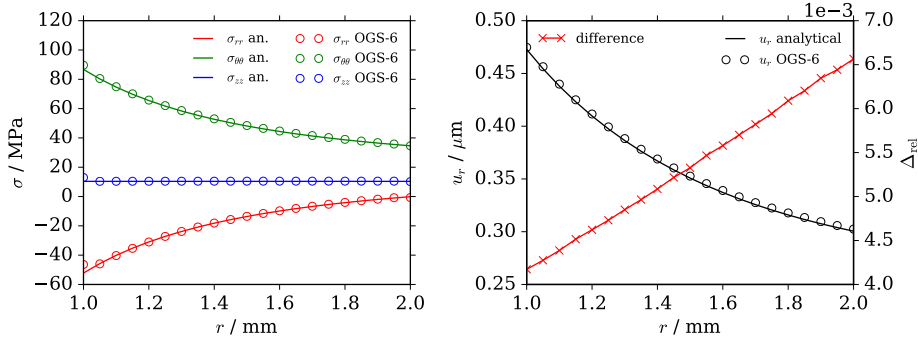


Figure 1: Plain strain elastic cylinder comparison between numerical and analytical results.

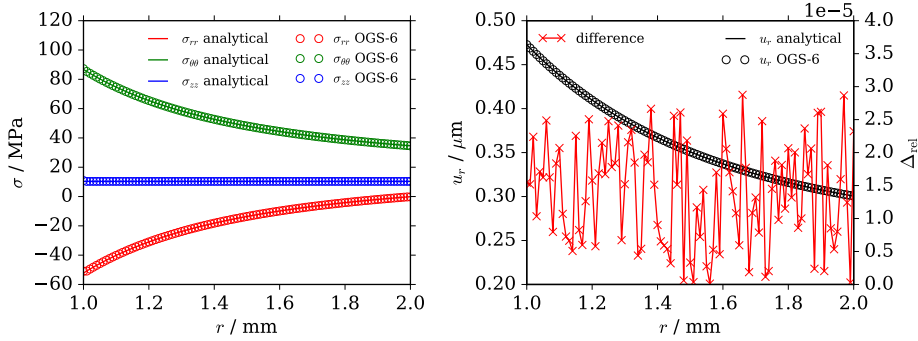


Figure 2: Axisymmetric elastic cylinder comparison between numerical and analytical results.

2.2. Elastic sphere

The comparison is carried out for the case of an elastic sphere of which properties are reported in Table 2.2. Two models are used for the numerical computations, a bi-dimensional axisymmetric one and a full tri-dimensional model. Results comparison for the axisymmetric model are reported in Figure 3 and for the tri-dimensional one in Figure 4. There is good agreement between numerical computations and the analytical solution. The slight discrepancy at the inner boundary is caused by nodal interpolation error.

Table 2: Values of parameters for elastic sphere problem.

| Parameter | Value | Units |
|-----------|-------|-------|
| R_i | 1 | mm |
| R_a | 2 | mm |
| p_i | 1 | kPa |
| p_a | 100 | kPa |
| ν | 0.35 | - |
| E | 125 | GPa |

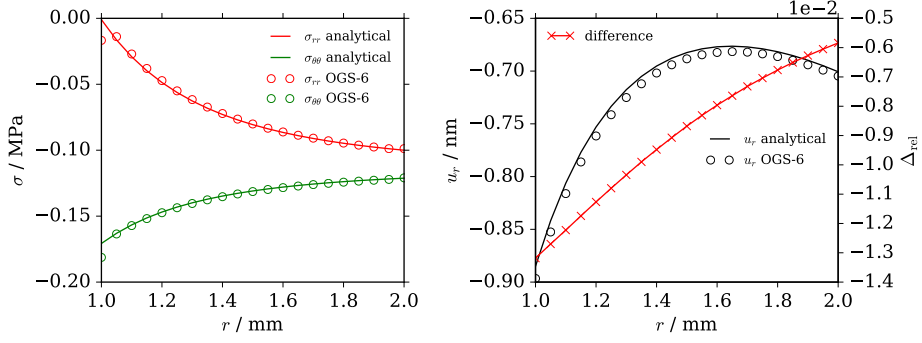


Figure 3: Axisymmetric elastic sphere comparison between numerical and analytical results.

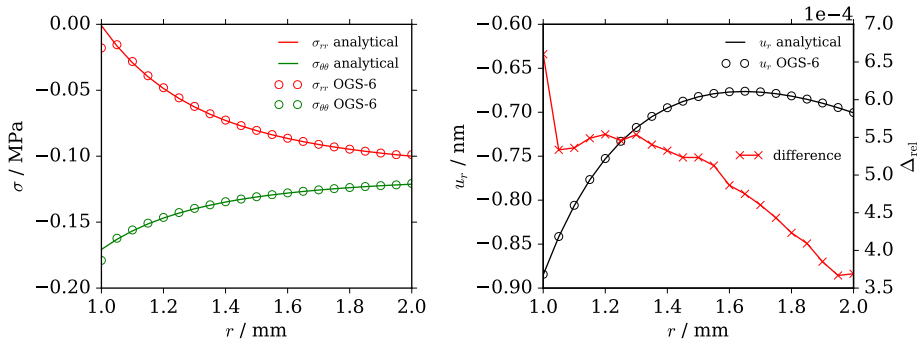


Figure 4: Tri-dimensional elastic sphere comparison between numerical and analytical results.

2.3. Plastic sphere

The final benchmarks consists in simulating an elasto-plastic sphere subjected to an internal pressure. The material properties, geometry and boundary conditions are reported in Table 2.3. The plastic radius r_p was set to be at the middle point of the sphere wall thickness. Based on this value, through Equation 9 the plastic stress p_{pl} was computed. In the numerical analysis, the internal pressure was increased linearly to the value of the computed plastic pressure p_{pl} . Results comparison are shown in Figure 5 and once again, the numerical solution well compares to the analytical one, validating the pressure boundary conditions implementation in OGS-6.

Table 3: Values of parameters for plastic sphere problem.

| Parameter | Value | Units |
|------------|--------|-------|
| R_i | 1 | mm |
| R_a | 2 | mm |
| p_i | 239.27 | MPa |
| p_a | 0 | MPa |
| ν | 0.35 | - |
| E | 125 | GPa |
| σ_F | 200 | MPa |
| r_p | 1.5 | mm |
| p_{pl} | 239.27 | MPa |
| E | 125 | GPa |

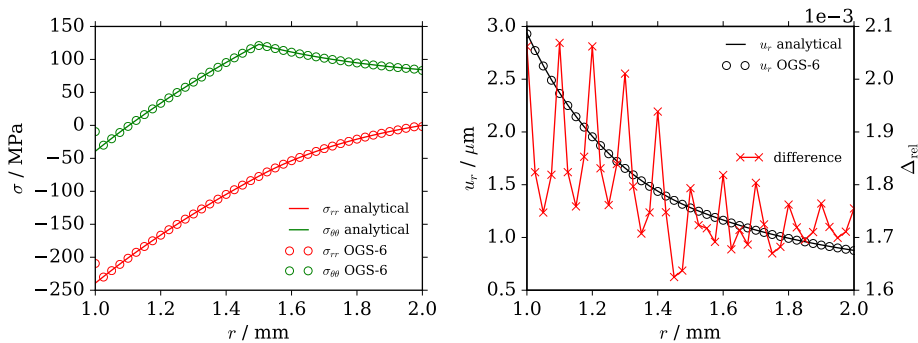


Figure 5: Axisymmetric plastic sphere comparison between numerical and analytical results.

We note that, as for the previous comparison in elastic condition, a greater discrepancy in the stress field between numerical and analytical solution is found at the inner boundary. Part of this is explained by the interpolation of quantities that are computed at integration points of the mesh (stress tensor): an error occurs during nodal interpolation. This discrepancy is mostly related to the fact that currently pressure boundary conditions are applied to the linearized normal of the boundary, and not to the true non-linear geometry. This is illustrated in Figure ??, in which the interpolation error for the case of the plastic sphere is shown. Future developments will include non-linear pressure boundary conditions and integration point output.

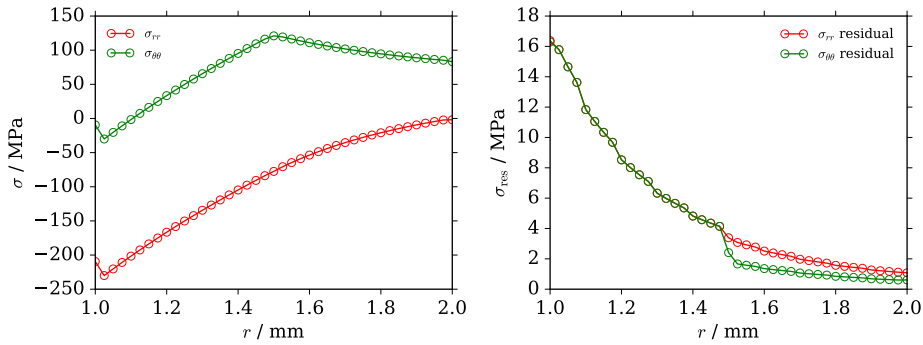


Figure 6: Axisymmetric plastic sphere: numerical results on the left and interpolation residuals of stress on the right.

3. Bibliography

- [1] O. Kolditz, H. Shao, W. Wang, S. Bauer, Thermo-hydro-mechanical-chemical processes in fractured porous media: modelling and benchmarking, Springer, 2016.